I&EC research
Industrial & Engineering Chemistry Research

Article

Cite This: Ind. Eng. Chem. Res. 2018, 57, 11195−11209

pubs.acs.org/IECR

The Role of Polyfunctionality in the Formation of [Ch]Cl-Carboxylic Acid-Based Deep Eutectic Solvents

Emanuel A. Crespo,[†,‡] Liliana P. Silva,[†] Mónia A. R. Martins,[†,§,∥] Mark Bülow,[‡] Olga Ferreira,[§,∥] Gabriele Sadowski,[‡] Christoph Held,[‡] Simão P. Pinho,[§,∥] and João A. P. Coutinho*[,†]

[†]CICECO − Aveiro Institute of Materials, Department of Chemistry, University of Aveiro, 3810-193 Aveiro, Portugal

[‡]Laboratory of Thermodynamics, Department of Biochemical and Chemical Engineering, TU Dortmund, 44227 Dortmund, Germany

[§]Associate Laboratory LSRE-LCM, Department of Chemical and Biological Technology and [∥]Mountain Research Center - CIMO, Polytechnic Institute of Bragança, 5301-857 Bragança, Portugal

Supporting Information

ABSTRACT: Aiming at providing an extensive characterization of the solid−liquid equilibria (SLE) of deep eutectic solvents (DESs), the phase diagrams of nine eutectic mixtures composed of choline chloride ([Ch]Cl) and (poly)carboxylic acids, commonly reported in the literature as DESs, were measured experimentally. Contrarily to the behavior reported for eutectic mixtures composed of [Ch]Cl (hydrogen-bond acceptor, HBA) and monofunctional hydrogen-bond donors (HBD) such as fatty acids and fatty alcohols, which have recently been shown to be almost ideal mixtures, a significant decrease of the melting temperature, at the eutectic point, was observed for most of the systems studied. This melting temperature depression was attributed to a pronounced nonideality of the liquid phase induced by the strong hydrogen-bond interactions between the two mixture components. Perturbed-chain statistical associating fluid theory (PC-SAFT) was used to describe these interactions physically. PC-SAFT allowed accurately modeling the experimental phase diagrams over the entire concentration and temperature ranges. Depending on the kind of mixture, up to two temperature-independent binary interaction parameters between HBA and HBD were applied. The PC-SAFT approach was used to provide trustworthy information on the nonideality of the liquid phase (expressed as the activity coefficients of HBA and HBD) as well as to estimate the eutectic points coordinates. The experimental data along with the modeling results allowed us to infer about the importance of the HBD's chemical structure on the formation of [Ch]Cl-based DESs.

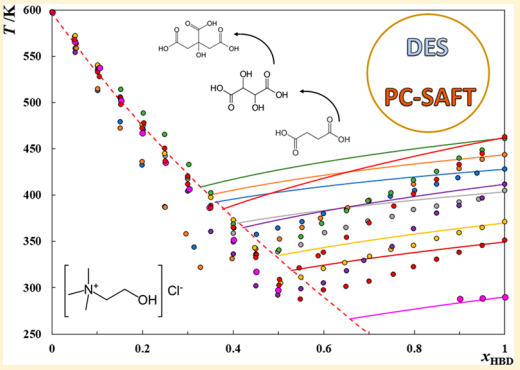

1. INTRODUCTION

The growing level of environmental awareness has been leading to a burgeoning focus on green chemistry. In this regard, one important research area is the synthesis and development of greener solvents for a wide number of industrial applications that still make use of classical organic solvents. The most prevalent green solvents studied nowadays include water, supercritical carbon dioxide (CO_2), ionic liquids (ILs), and in the past decade, deep eutectic solvents (DESs).

According to Abbott and co-workers,[1] DESs are a neoteric class of eutectic solvents obtained by mixing two (or more) compounds that exhibit a eutectic temperature far below the melting points of the starting materials, resulting in stable liquids at low temperatures.[2] They assigned this behavior to the charge delocalization induced by strong hydrogen-bonding interactions established between a hydrogen bond donor (HBD) and a hydrogen bond acceptor (HBA) (stronger interactions inducing larger melting temperature depressions).

DESs are usually described as solvents with low toxicity, nonflammability, water compatibility, and negligible vapor pressure. Moreover, their simple preparation, operation under mild conditions, low cost, biodegradability, and sustainability are often highlighted.[2,3] Although some of these characteristics may be arguable as, for instance, their "low toxicity",[4−6] DESs have emerged as a promising alternative to organic solvents, breaching a new field of research. The most worthwhile feature of DESs is, analogously to ILs, their tunable character. This means that the phase behavior and physical properties of the solvent can be tuned aiming at a specific application, by a proper selection of HBD/HBA combinations.[7] The most common DES precursors consist of quaternary ammonium salts (mainly choline chloride ([Ch]Cl), due to its low cost,

Received: March 21, 2018
Revised: July 12, 2018
Accepted: July 19, 2018
Published: July 19, 2018

DOI: 10.1021/acs.iecr.8b01249
Ind. Eng. Chem. Res. 2018, 57, 11195−11209

low toxicity, and biodegradability) as HBAs, combined with different harmless HBDs such as urea and its derivatives,[1,8] sugars,[9] alcohols or polyols,[10−12] carboxylic acids,[12−16] or amino acids.[17,18]

Recently, many possible applications for DESs have emerged in several research fields such as organic synthesis or catalysis,[19−21] metal processing,[22] conversion of lignocellulosic biomass,[23] extraction of glycerol from biodiesel,[24,25] drug vehicles,[8] and gas separations.[26] A reliable knowledge of thermophysical properties and phase equilibria of the DES are necessary for the accurate simulation and/or design of novel industrial processes. However, the mechanisms behind the formation of a DES are still not fully understood, hindering the development of theoretical models able to correctly capture their thermophysical properties and phase equilibria.

In previous works,[12,16] we characterized the solid−liquid equilibria (SLE) of several eutectic mixtures composed of monofunctional HBD's, namely, alkan-1-ols and monocarboxylic acids, combined with quaternary ammonium salts. The phase diagrams were experimentally measured and modeled using the equation of state perturbed-chain statistical associating fluid theory (PC-SAFT)[27,28] or the nonrandom two liquid (NRTL) model. PC-SAFT showed to be the most appropriate given its higher accuracy, and contrarily to NRTL, it can provide densities or be easily coupled with other theories for the calculation of transport or interfacial properties in subsequent studies. By and large, the results showed that, although commonly reported as DES, most of these systems do not show significant deviations from the ideal-mixture behavior and consequently exhibit low melting temperature depressions. Furthermore, no fixed stoichiometry between the HBD and the HBA was observed. Instead, it was shown that the eutectic composition varies depending on the precursors used, being mainly driven by the HBD's melting properties.

These results reinforce the need for further investigations on the DESs nature. This is of special importance as the literature reports a large number of DESs and their numerous applications while experimental data on their SLE are extremely scarce despite the fundamental information they can provide.

Likewise, the thermodynamic modeling of DESs is a poorly explored research topic. The reason behind this is caused by the limited reliable data available and the complexity of the DESs; for these systems hydrogen-bonding or polar interactions play an important role, which remains challenging for most industrially relevant thermodynamic models currently available.[29]

Promising molecular-based equations of state (EoSs), able to explicitly account for specific molecular interactions such as hydrogen-bonding, have been derived from statistical associating fluid theory (SAFT). Verevkin et al.[30] predicted the separation performance of DESs when compared to their parent ionic liquids, by using PC-SAFT to describe the infinite dilution activity coefficients of several solutes in a [Ch]-Cl:glycerol mixture. Zubeir et al.[31] also used PC-SAFT to describe the phase behavior of DESs composed of quaternary ammonium salts and lactic acid in order to predict the solubility of CO_2 in them. Two PC-SAFT modeling approaches, the pseudopure component approach and the individual-component approach were considered and compared. The latter allowed binary interaction parameters to be HBD:HBA ratio independent, which is a big advantage compared to applying the pseudopure component approach. Lloret et al.[32] used soft-SAFT to study the thermophysical properties of DESs composed of tetraalkylammonium chlorides as HBAs and lactic acid, ethylene glycol, or triethylene glycol as HBDs. In their work, density and phase equilibria with CO_2 were modeled using the pseudopure component and the individual-component approaches. However, the viscosities and surface tensions of the DESs were modeled only with the pseudopure component approach. Although the pseudopure component modeling approach is easy, the most relevant limitation of this approach is its inability to investigate the solid−liquid (SL) phase behavior, which is of utmost importance for a fundamental knowledge on the DESs essence and to establish temperature and composition limits for practical operations.

In this work, the SL phase diagrams of nine binary mixtures composed of [Ch]Cl and different (poly)carboxylic acids, namely, glycolic, lactic, oxalic, malonic, succinic, glutaric, malic, tartaric, and citric acids were measured using a visual detection technique. The SLE phase diagrams were then described using PC-SAFT, which is able to explicitly account for hydrogen-bond interactions between the DES constituents. As the model provided a good description of the data, it was further considered to obtain reliable estimates for the nonideality of the liquid phase and for the eutectic points coordinates. The experimental data along with the modeling results were used to grasp the influence of the polyfunctionality of the HBD on the nonideality of the DES's liquid phase. Densities and viscosities of the different systems at compositions near the eutectic point were measured at different temperatures.

2. MATERIALS AND METHODS

2.1. Materials. The source and purity of the compounds investigated in this work are reported in Table 1. The racemic mixture DL-lactic acid was considered for this study despite its lower purity in order to provide a broader discussion on the influence of the acids structure on the SLE. Nevertheless, the acid was dried prior to use and, thus, the influence of water (the main impurity according with the supplier) was assumed to be negligible. The melting temperatures of the different carboxylic acids used in this work were measured experimentally and are reported in Table 1, along with values from literature. A good agreement between the experimental and literature melting temperatures (T_m) is observed with a maximum deviation of 4.1 K, for malonic acid. The melting enthalpies (ΔH^{sl}) were taken from literature and are also reported in Table 1. Before use, all individual compounds were purified under vacuum (0.1 Pa and 298 K) and constant stirring, for at least 72 h. The water content of the pure compounds was measured using a Metrohm 831 Karl Fischer coulometer, with the analyte Hydranal Coulomat AG from Riedel-de-Haen, and their values are displayed in Table 1.

2.2. Methods. Due to the high hygroscopic character of the pure compounds, their mixtures were prepared inside a dry-argon glovebox at room temperature using an analytical balance model ALS 220-4N from Kern with an accuracy of ±0.002 g. Mixtures were then heated under stirring until complete melting, recrystallized, and grounded inside the glovebox (Figure S1). The crystallization times for the pasty compounds were about 12 h with the exception of the mixture involving citric acid that starts to crystallize upon cooling. The obtained powder was filled into a glass capillary. The melting temperatures were determined using an automatic glass capillary device model M-565 by Bucchi (100−240 V, 50−

DOI: 10.1021/acs.iecr.8b01249
Ind. Eng. Chem. Res. 2018, 57, 11195−11209

Table 1. Source, Purity, and Melting Properties of the Chemicals Used in This Work

Compound	Source	%wt	H_2O/ppm	T_m/ K exp.	T_m/ K lit.	ΔH^{fl} / J·mol^{-1}	Chemical Structure
[Ch]Cl	Acros Organics	98	639	-	597[33]	4300[33]	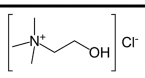
Glycolic acid	Sigma-Aldrich	99	148	350.8 ± 0.2	351.3[34]	19300[34]	
DL - Lactic acid	Riedel de Haen	88	523	289.8 ± 0.3	289.9[35]	11340[35]	
Oxalic acid	JMGS	99	363	462.4 ± 0.3	462.6[36]	18580[36]	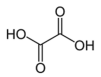
Malonic acid	Fluka	>98	531	411.6 ± 0.4	407.5[37]	23100[37]	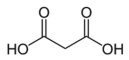
Succinic acid	Merck	99	463	460.7 ± 0.2	460.1[38]	32950[38]	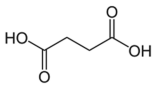
Glutaric acid	Sigma	99	584	370.6 ± 0.2	370.9[39]	20700[39]	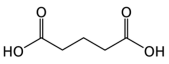
Malic acid	Riedel de Haen	99.5	579	404.3 ± 0.1	402[40]	33522[40]	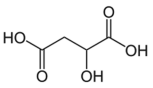
Tartaric acid	Acros Organics	99.5	492	443.3 ± 0.2	445.0[41]	36310[41]	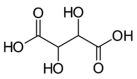
Citric acid	Fisher Scientific	100	112	427.5 ±0.3	427.8[41]	40320[41]	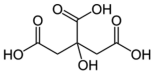

60 Hz, 150 W) with a temperature resolution of 0.1 K. A heating rate of 0.1 K·min^{-1} was used in all cases.

For mixtures with a paste-like consistency (Table S1), the vials (5 mL size with approximately 0.3 g of sample) were gradually heated under stirring in an oil bath until a homogeneous liquid was formed, the mixture melting point. The temperature was controlled and measured with a PT100 probe with a precision of ±0.1 K. The probe was previously calibrated against a calibrated platinum resistance thermometer, SPRT100 (Fluke-Hart Scientific 1529 Chub-E4), traceable to the National Institute of Standards and Technology (NIST), with an uncertainty less than 2×10^{-2} K. The heating rate used was of 1 K·min^{-1}. The melting procedures were repeated at least three times with an estimated reproducibility of ±1.5 K.

The water content of the eutectic points of the investigated mixtures was measured after melting using a Metrohm 831 Karl Fischer coulometer, with the analyte Hydranal-Coulomat AG from Riedel-de Haën (Table S2). The water content of the mixtures after melting is higher than the water content of the mixtures' pure components (Table 1). This increase is expected due to the hygroscopic character of choline chloride.

Mixtures were analyzed by nuclear magnetic resonance (NMR) spectroscopy at room temperature 24 h after their formation (Figure S2) using a Bruker Avance 300 equipment operating at 75 MHz. Dimethyl sulfoxide (DMSO) was used as solvent and (trimethylsilyl)propanoic acid (TSP) as internal reference. No significant differences in the spectra or new NMR signals were observed 24 h after the formation of the systems, showing that esterification does not significantly affect the SLE measurements. However, it is important to point out that long-term usage of these mixtures at elevated temperatures might lead to significant esterification.

Densities and viscosities were measured at atmospheric pressure and in the temperature range from 283.15 to 373.15 K using an automated SVM 3000 Anton Paar rotational Stabinger viscometer−densimeter (temperature uncertainty, ±0.02 K; absolute density uncertainty, $\pm 5 \times 10^{-4}$ g·cm^{-3}; dynamic viscosity relative uncertainty, ±0.35%)

3. THEORETICAL BACKGROUND

3.1. PC-SAFT. Cubic equations of state (EoSs) used in industry often fail when applied to describe the thermodynamic behavior and phase equilibria of complex systems where hydrogen-bonding and/or polar interactions play a key role. Due to an ever-increasing number of complex systems of interest to the chemical industry, there is an ongoing demand for more robust and accurate thermodynamic models suitable for broader ranges of applications.

Therefore, although still relatively far from becoming the standard for engineering purposes,[42] molecular-based EoSs having a strong theoretical foundation derived from statistical thermodynamics and able to explicitly account for physical, chain, and association interactions have emerged as the most encouraging alternative to model associating fluids such as DESs. SAFT provides such a concept; it was first implemented as an engineering EoS by Chapman and co-workers[43] in the late 80s based on the first-order thermodynamic perturbation theory (TPT1) proposed by Wertheim.[44−47]

Instead of hard spheres as a reference fluid, PC-SAFT considers a hard chain of freely jointed hard spheres, as reference for the perturbation theory, rather than the individual spherical segments.[27,28] Thus, for PC-SAFT the residual Helmholtz energy, A^{res} can be expressed by eq 1 where hc refers to the hard-chain contribution:

$$\frac{A^{res}}{Nk_BT} = \frac{A^{hc}}{Nk_BT} + \frac{A^{disp}}{Nk_BT} + \frac{A^{assoc}}{Nk_BT} \quad (1)$$

The hard-chain reference fluid chosen as reference in PC-SAFT, consists of a number of m_i^{seg} spherical freely jointed segments (no attractive interactions) accounting for the nonspherical shape of molecules and the repulsive interactions.

The contribution due to dispersive interactions within PC-SAFT is derived from the perturbation theory of Barker and Hendersen[48,49] and includes two additional parameters, namely, the segment diameter (σ_{ii}) and dispersive energy between segments $\left(\frac{u_{ii}}{k_B}\right)$. These two parameters along with the number of segments in the chain (m_i^{seg}) are the nonassociative parameters required to fully characterize a nonassociating compound. The size and energy parameters required in the dispersive term for mixtures are obtained under the van der Waals one fluid theory (vdW1) using the Lorentz−Berthelot mixing rules (eqs 2 and 3).

$$\sigma_{ij} = \frac{\sigma_{ii} + \sigma_{jj}}{2} \quad (2)$$

$$u_{ij} = (1 - k_{ij})\sqrt{u_{ii}u_{jj}} \quad (3)$$

The association term introduces two additional parameters, namely, the association well depth (ε^{kilj} or ε^{HB}) and association volume (κ^{kilj} or κ^{HB}) that, along with the three nonassociating

DOI: 10.1021/acs.iecr.8b01249
Ind. Eng. Chem. Res. 2018, 57, 11195−11209

Table 2. Molar Mass, Number of Sites, and PC-SAFT Pure-Component Parameters Used in This Work

component	M_w/(g·mol^{-1})	no. of sites A/B	m_i^{seg}	σ_i/Å	u_i/K	$\varepsilon^{A_iB_i}$/K	$\kappa^{A_iB_i}$	%AARD(p)
[Ch]Cl[31]	139.62	1/1	13.02	2.368	228.07	8000	0.200	
glycolic acid[a]	76.05	2/2	3.609	2.914	261.44	1850	0.020	6.03
lactic acid[31]	90.08	1/1	4.080	2.851	275.53	100.2	0.001	
oxalic acid[36]	90.04	2/2	3.358	2.749	180.14	1655	0.02	
malonic acid[a]	104.06	2/2	4.428	2.818	330.16	2125	0.023	0.34
succinic acid[60]	118.09	2/2	4.335	3.055	477.44	1702	0.020	
glutaric acid[59]	132.12	2/2	4.437	2.799	257.67	1762	0.020	
malic acid[a]	134.09	3/3	4.611	2.987	204.83	3163	0.027	3.16
tartaric acid[a]	150.09	4/4	7.637	2.532	204.56	2963	0.040	0.33
citric acid[a]	192.12	4/4	8.546	2.723	227.18	2488	0.044	2.25

[a]Parameters regressed in this work.

parameters, fully describe a self-associating component, as those present in DESs.

The extension of the association term to mixtures requires the evaluation of the cross-association parameters, which are generally obtained from the pure-component association parameters using appropriate mixing rules such as those of Wolbach and Sandler:[50]

$$\varepsilon^{kilj} = \frac{1}{2}(\varepsilon^{kiki} + \varepsilon^{ljlj})(1 - k_{ij\_eps}) \tag{4}$$

$$\kappa^{kilj} = \sqrt{\kappa^{kiki}\cdot\kappa^{ljlj}}\left(\frac{\sqrt{\sigma_{ii}\cdot\sigma_{jj}}}{1/2(\sigma_{ii} + \sigma_{jj})}\right)^3 \tag{5}$$

For further details on the PC-SAFT EoS and its implementation, we refer to the original PC-SAFT publications by Gross and Sadowski.[27,51]

One clear advantage of an EoS written in terms of the Helmholtz free energy is that the derivation of all the thermodynamic properties is possible using derivatives and ideal-gas integrals. Therefore, the compressibility factor, residual chemical potentials, and fugacity coefficients required to perform phase equilibria calculations can be obtained using the following equations:

$$Z = 1 + \eta\left(\frac{\partial\tilde{a}^{res}}{\partial\eta}\right)_{T,x_i} \tag{6}$$

$$\frac{\mu_k^{res}(T,Vm)}{RT} = \tilde{a}^{res} + (Z - 1) + \left(\frac{\partial\tilde{a}^{res}}{\partial x_k}\right)_{T,Vm,x_{i\neq k}} - \sum_{j=1}^{NC}\left(x_j\left(\frac{\partial\tilde{a}^{res}}{\partial x_j}\right)_{T,Vm,x_{i\neq j}}\right) \tag{7}$$

$$\ln(\varphi_k) = \frac{\mu_k^{res}(T,V_m)}{RT} - \ln(Z) \tag{8}$$

where $\tilde{a}^{res}$ is the molar residual Helmholtz energy, V_m is the molar volume, η is the reduced density, Z is the compressibility factor, μ_k^{res} is the residual chemical potential of component k, and φ_k is its fugacity coefficient.

3.2. PC-SAFT Pure-Component Parameters. The pure-component parameters required for PC-SAFT modeling are generally regressed from pure-component experimental data (saturated liquid densities and vapor pressures in the 0.4−0.9 reduced temperature range are used in most cases). However, for compounds that are solid at low temperatures, as is the case of [Ch]Cl and most of the (poly)carboxylic acids investigated here, liquid densities are not available and their pure-component parameters need to be regressed either from vapor pressure data only or from binary VLE or LLE data with a solvent for which parameters are readily available (e.g., water). Both approaches have their shortcomings: using only vapor pressure data would mean regressing up to five parameters from experimental data corresponding to a single thermodynamic property while, in the latter approach, the obtained parameters may be strongly influenced by the mixtures physical features and a binary interaction parameter may be simultaneously fitted so that a quantitative agreement is obtained.

These problems can, in some cases, be mitigated as the associative parameters may be transferable within a homologous series of compounds where the same kind of interactions are present. However, the (poly)carboxylic acids investigated here differ from each other by different chain lengths and by different numbers of hydroxyl and carboxylic groups in their molecular structure (Table 1), which may prevent a successful transfer of associative parameters between the acids.

When PC-SAFT parameters for self-associating components are regressed, exceptional care is needed since the number and type of association sites of a molecule, as well as the possible site-to-site interactions, need to be specified a priori; these might have a tremendous impact on the modeling results. These "association schemes" should be carefully chosen on the basis of the molecular picture and known interactions, as NMR spectroscopy data are rarely available.

In the framework of PC-SAFT, several authors[16,31,52−54] have represented salts and ionic liquids as associative compounds using a 2B association scheme (according to Huang and Radosz[55]). 2B means that two association sites (one donor and one acceptor) are assigned to the considered component, while allowing for unlike interactions in the system. Regarding the components in the present work, pure-component parameters for [Ch]Cl with the 2B scheme were already available from the work of Zubeir et al.[31] (as reported in Table 2); these were directly used also in the present work.

For the modeling of carboxylic acids, both the 1A and 2B association schemes were previously considered in the literature, and the 2B scheme (the same applied to alkan-1-ols) was suggested as the more appropriate.[16,56,57] As some of the (poly)carboxylic acids studied here contain both carboxylic and hydroxyl groups (hydroxy acids), two association sites (of different nature as in the 2B scheme) are added per each one of these groups. A sketch of the resulting association scheme

DOI: 10.1021/acs.iecr.8b01249
Ind. Eng. Chem. Res. 2018, 57, 11195−11209

for citric acid is presented in Figure 1, where the A and B notation are used to differentiate association sites of opposite

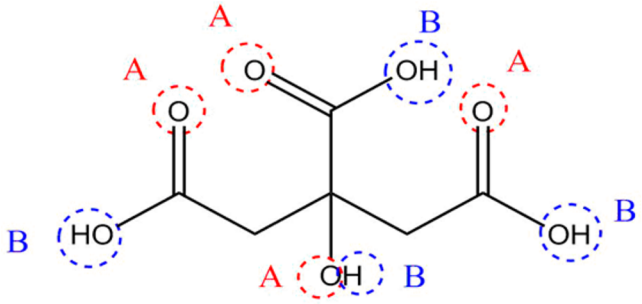

Figure 1. Association scheme 4/4 proposed for citric acid.

nature; among two equal components as well as between two unlike components, only A and B are allowed to interact.

As mentioned above, the different molecular structures of the (poly)carboxylic acids hinder the transferability of association parameters and, thus, the five pure-component parameters for glycolic, malonic, malic, tartaric, and citric acids were regressed from pure-compound vapor pressure data, where the quality of the fit is depicted in Figure 2, along with one density point whenever available according to Table 3. As depicted in Figure 2, the parameters obtained allowed for a good description of the experimental data and are reported in Table 2, along with the percentage average absolute relative deviation (%AARD) to the experimental vapor pressures. The highest deviation was observed for glycolic acid for which no experimental vapor pressure data in an appropriate temperature range (experimental data in the 0.4−0.9 range of reduced temperatures is usually used for the fitting) are available in the literature. Instead, vapor pressure data estimated using the Riedel's method[58] were considered. Emel'Yanenko et al.[34] measured the glycolic acid's sublimation pressures; however, the experimental measurements were carried in a very small temperature range and at very low temperatures (323−343 K).

The regression of the parameters for (poly)carboxylic acids from binary LLE data was also attempted for citric, malonic, and malic acids for which solubility data in different organic solvents (such as ethanol, acetonitrile, 2-propanol, THF, and 1,4-dioxane) were available. However, although reasonable results were obtained for the LLE, a binary interaction parameter was required to describe each binary mixture. Taking this into account and because the LLE data were not available for all the (poly)carboxylic acids studied, the PC-SAFT parameters were finally obtained by the first approach, i.e., fitted to vapor pressure data and density data of the pure (poly)carboxylic acids. PC-SAFT parameters for lactic, oxalic, succinic, and glutaric acids were available from previous works;[31,36,59,60] these were directly used also in this work.

3.3. Solid−Liquid Equilibria. It can be demonstrated that the solubility of a solid solute $k(x_k)$ in a liquid solvent can be given by the following simplified expression:[62]

$$x_k\gamma_k^{l} = \exp\left\{\left(\frac{\Delta H_k^{sl}}{RT_{mk}}\right)\frac{T - T_{mk}}{T} + \frac{\Delta C_{p_k}^{sl}}{R}\left[\ln\left(\frac{T}{T_{mk}}\right) - \frac{T - T_{mk}}{T}\right] + I\right\} \quad (9)$$

where γ_k^{l} is the activity coefficient of component k in the liquid phase, ΔH_k^{sl} and T_{mk} are, respectively, the melting enthalpy and temperature of pure component k, T is the system absolute temperature, R is the ideal-gas constant, ΔC_{pk}^{sl} is the heat-capacity change of melting, and I is a triple integral for a second-order contribution, normally neglected.

This equation assumes that the solid phases of each individual component are immiscible and crystallize independently as expected from a eutectic-type phase diagram. Moreover, the term containing the heat-capacity change upon melting can be significant,[63] in particular for systems where the melting enthalpies are small and temperatures are very far from the melting temperature of the pure compounds, but experimental values are usually unavailable. For the (poly)carboxylic acids the term has no or little influence, while for [Ch]Cl Martins et al.[63] recently presented a detailed analysis over a large number of different binary systems with [Ch]Cl concluding that the heat-capacity change in most cases has no relevant influence.

Therefore, assuming that I and ΔC_{pi}^{sl} are negligible eq 9 can be further simplified:

$$x_k\gamma_k^{l} = \exp\left[\left(\frac{\Delta H_k^{sl}}{RT_{mk}}\right)\frac{T - T_{mk}}{T}\right] \quad (10)$$

According to eq 10, the solubility of a solid solute can be easily obtained as a function of the solute melting properties, temperature and composition of the liquid phase. The activity coefficients of a component k in the liquid phase, which are a function of temperature and composition, are obtained from an EoS as the ratio between the fugacity coefficients of component k in the mixture and that of the pure compound, as follows:

$$\gamma_k^{l}(T,P,x) = \frac{\varphi_k^{l}(T,P,x)}{\varphi_{ok}(T,P,x_k = 1)} \quad (11)$$

Equation 9 neglects the existence of any solid−solid transitions, but some of the studied components do show polymorphic behavior. According to the literature, five of the compounds studied in this work present solid−solid transitions, namely, [Ch]Cl,[64,65] oxalic,[66] malonic,[35,66,67] succinic,[35] and glutaric acids.[35,66,68]

For [Ch]Cl there are no values of the transition enthalpy reported in literature while for succinic acid the transition temperature is lower than the eutectic point of the binary system [Ch]Cl + succinic acid. For the remaining acids, the solid−solid transitions were not included given that the transition enthalpies typically reported are within the uncertainty of the fusion enthalpy.

Hence, given the scarcity and uncertainty of the solid−solid transition temperatures and enthalpies, it is yet inadequate to explicitly account for them in eq 9.

4. RESULTS

The nine solid−liquid phase diagrams measured in this work for binary mixtures composed of [Ch]Cl and (poly)carboxylic acids are depicted in Figure 3. All phase diagrams exhibit a phase behavior characterized by a single eutectic, as commonly observed for most crystallizing systems. The detailed SLE data are reported in the Supporting Information (Table S1) along with the experimental activity coefficients calculated through

DOI: 10.1021/acs.iecr.8b01249
Ind. Eng. Chem. Res. 2018, 57, 11195−11209

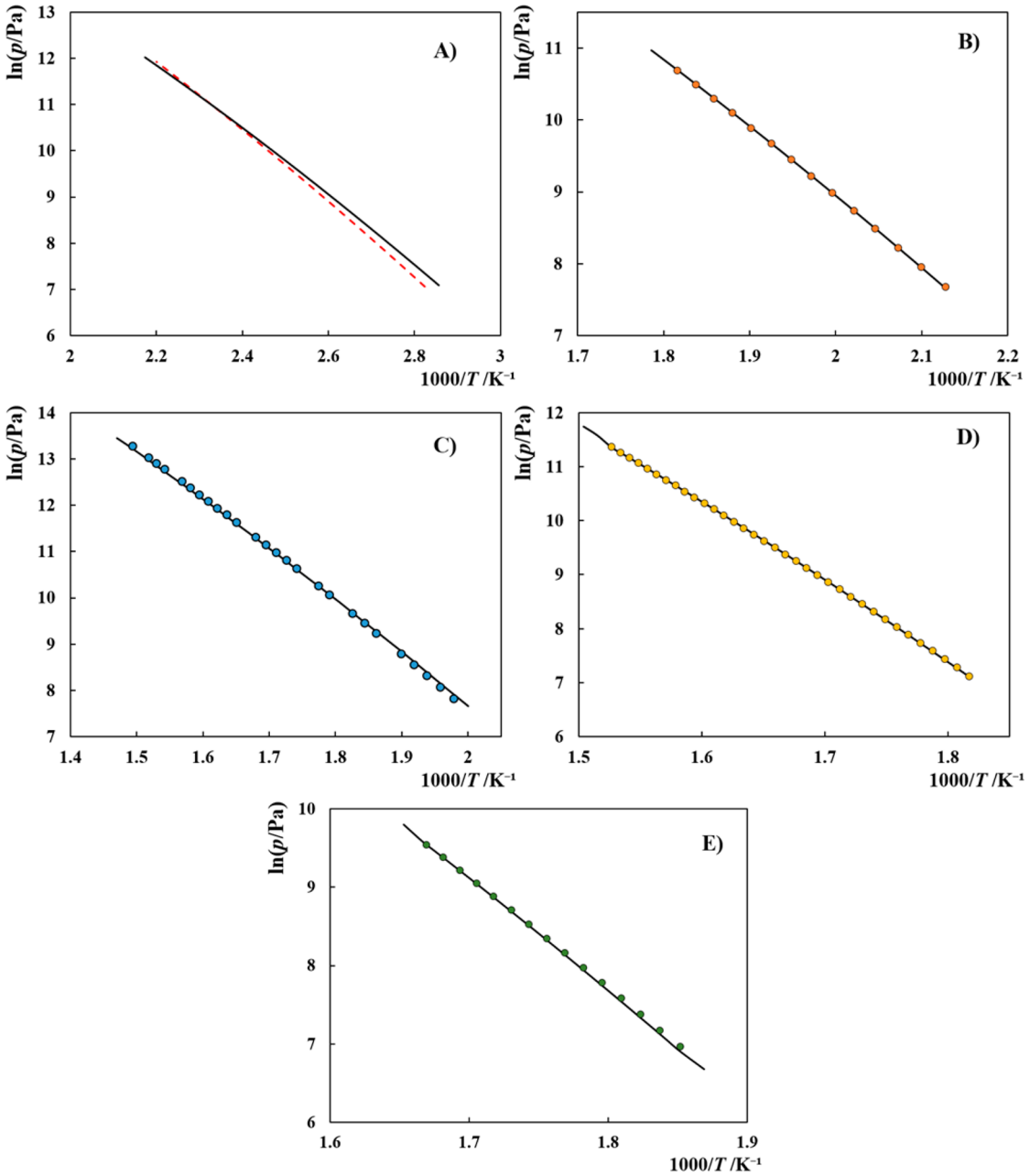

Figure 2. Vapor pressures of (poly)carboxylic acids: (A) glycolic acid, (B) malonic acid, (C) malic acid, (D) tartaric acid, and (E) citric acid. Symbols represent the experimental data[61] while solid lines depict the PC-SAFT results using the parameters from Table 2. Data estimated from Riedel's equation are represented by a red dashed line.

Table 3. Densities of Some Acids Considered in the Fitting Procedure

component	T/K	ρ^{exp}/(kg·m^{-3})	ρ^{calc}/(kg·m^{-3})	%AARD
malonic acid[a]	104.06	1619.0[61]	1619.6	0.038
tartaric acid[a]	150.09	1788.0[61]	1790.7	0.151
citric acid[a]	192.12	1664.9[61]	1665.3	0.019

[a]Parameters regressed in this work.

eq 10, using the solubility measurements (x, T) and melting data.

At some compositions, the mixture [Ch]Cl + lactic acid is liquid at room temperature. Thus, to measure the complete phase diagram, another experimental technique (differential scanning calorimetry) was used. However, these mixtures do not crystallize, forming glasses instead, preventing the measurement of the complete SLE phase diagram of the system [Ch]Cl-lactic acid.

Abbott et al.[13] reported the freezing temperatures for the systems [Ch]Cl + oxalic acid, [Ch]Cl + malonic acid, and [Ch]Cl + succinic acid in a small composition range. As depicted in Figure 3, near the eutectic point, the data from literature are in good agreement with those measured in this work. However, larger discrepancies are observed for higher concentrations of [Ch]Cl, which may be partly related to the hygroscopic character of this compound, as the higher the water content is, the lower is the melting temperature. The mixtures investigated here were carefully prepared and manipulated inside a dry-argon glovebox just right to introduce the mixture powder into the capillary tube, immediately before

DOI: 10.1021/acs.iecr.8b01249
Ind. Eng. Chem. Res. 2018, 57, 11195−11209

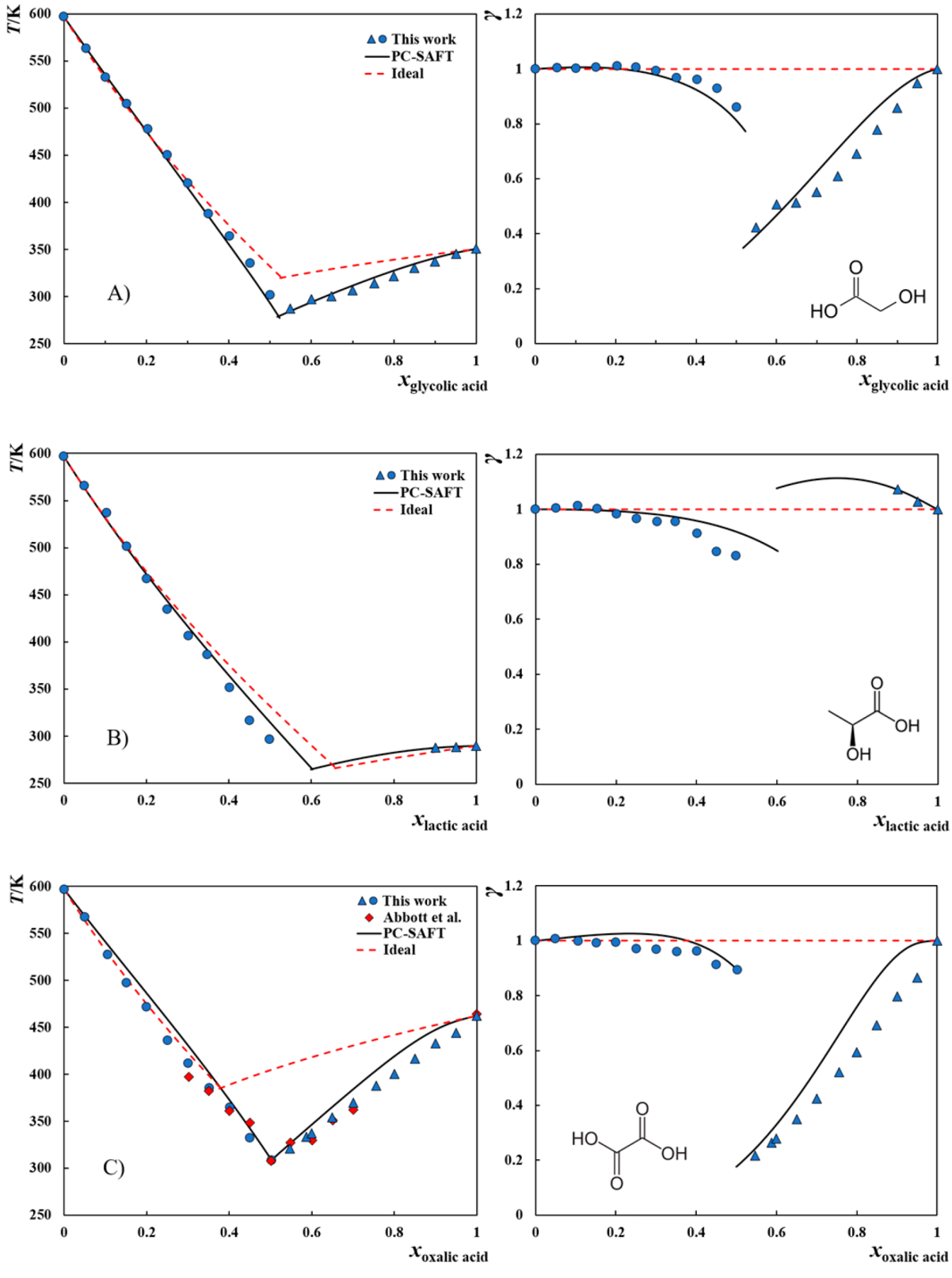

Figure 3. continued

DOI: 10.1021/acs.iecr.8b01249
Ind. Eng. Chem. Res. 2018, 57, 11195−11209

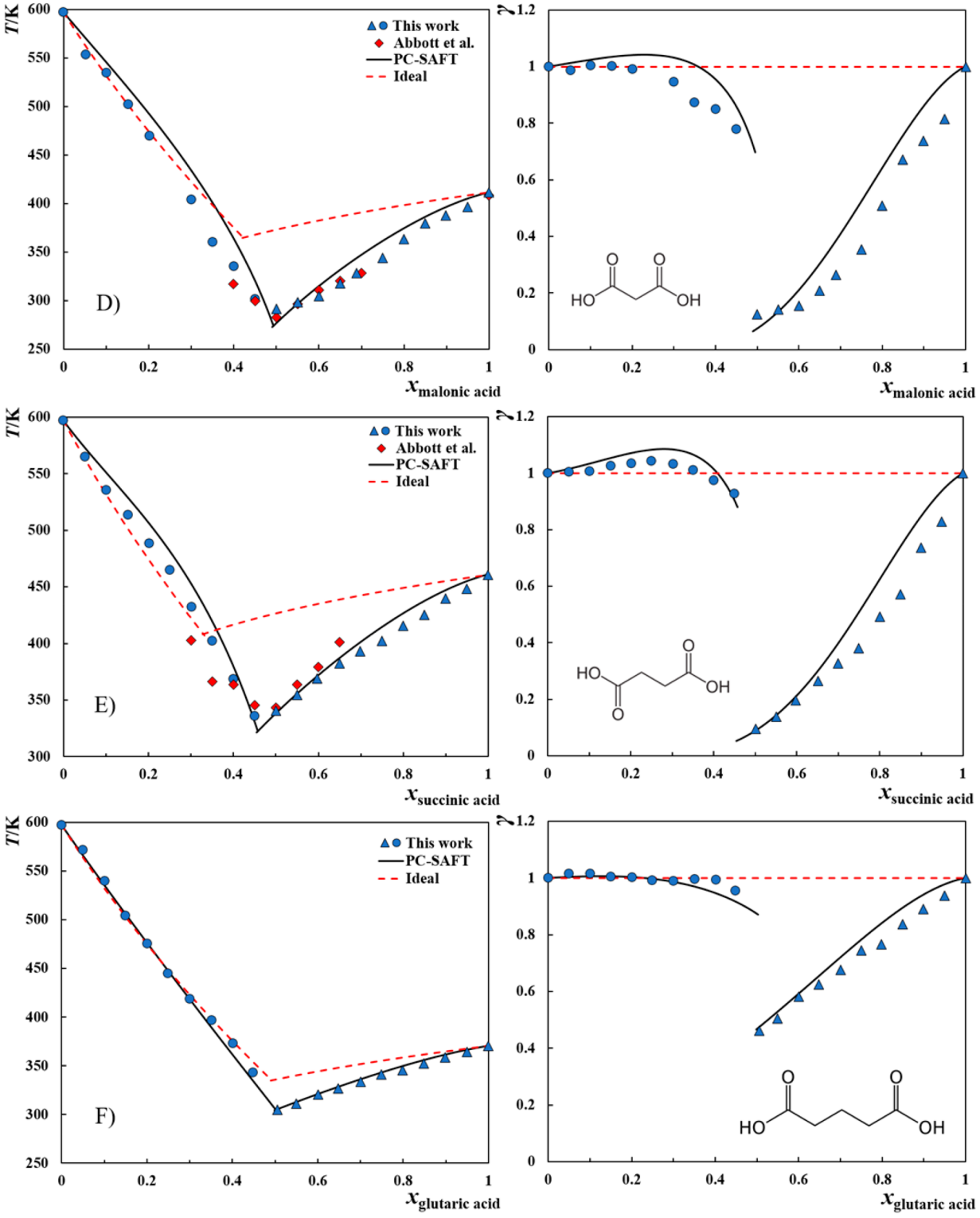

Figure 3. continued

DOI: 10.1021/acs.iecr.8b01249
Ind. Eng. Chem. Res. 2018, 57, 11195−11209

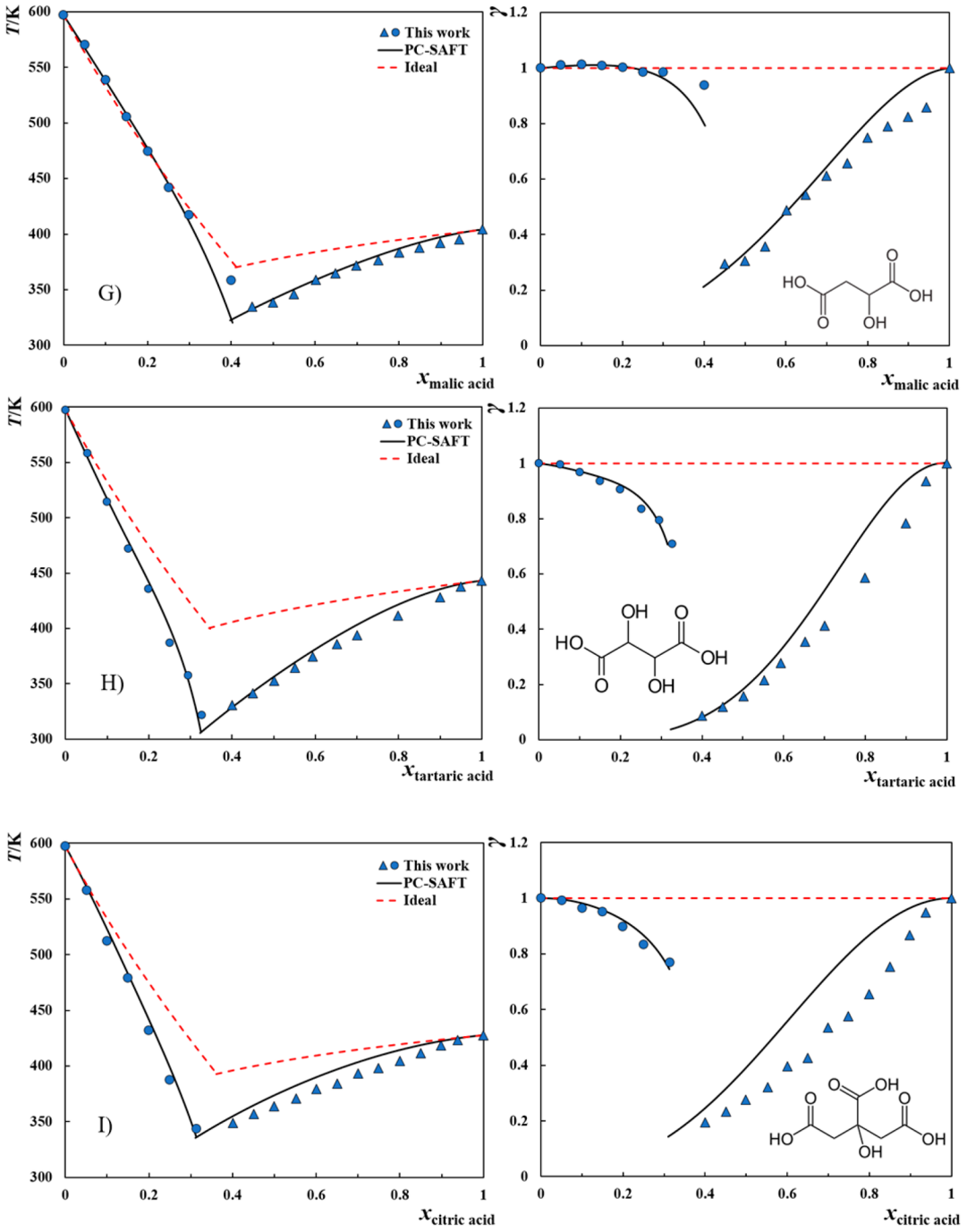

Figure 3. Solid−liquid phase diagrams (left side) for the binary mixtures composed of [Ch]Cl and different carboxylic acids. On the right side the activity coefficients of both species are shown. The symbols represent the experimental data of this work (see Table S1) while the solid lines depict the PC-SAFT results using the parameters from Table 2 and Table 4, and the dashed lines represent the ideal-mixture behavior.

the measurement of the melting temperature. Moreover, the pure components were dried before the mixtures preparation, being the water content always lower than 639 ppm (Table 1).

Assuming an ideal liquid phase (i.e., $\gamma_k^l = 1$), ideal solubility curves can be obtained from eq 10 as a function of the system temperature and the solute melting properties; these curves are also displayed in Figure 3, evidencing the presence of significant negative deviations from the ideal behavior, as the experimental melting temperatures are systematically lower than those calculated assuming an ideal behavior, especially for the acid solubility curve. For most systems, the [Ch]Cl solubility curves present smaller deviations from the ideal-mixture behavior, with activity coefficients close to 1, but the departure to ideality increases considerably for tartaric and citric acids. The reason behind this is probably the very high number of functional groups that are able to form hydrogen bonds with [Ch]Cl (four between hydroxyl and carboxylic groups). These results suggest that additional functional groups in the HBD's structure may play a vital role for inducing a higher nonideality in [Ch]Cl-based DESs. This assumption is supported by our previous work,[12] on mixtures of [Ch]Cl with monocarboxylic acids; these were shown to have a nearly ideal behavior, exhibiting very small deviations

DOI: 10.1021/acs.iecr.8b01249
Ind. Eng. Chem. Res. 2018, 57, 11195−11209

from ideal behavior, and often a negligible melting temperature depression.

Considering the nonideality of the systems investigated here, PC-SAFT was used to model the experimental phase diagrams and, as depicted in Figure 3, an accurate description of the experimental data was obtained by using up to two temperature independent binary interaction parameters (k_{ij} and k_{ij_eps}) (Table 4).

Table 4. PC-SAFT Model Binary Interaction Parameters Regressed from SLE Data

	PC-SAFT binary parameters	
system	k_{ij}	k_{ij_eps}
[Ch]Cl + glycolic acid	−0.0300	−0.0210
[Ch]Cl + lactic acid		
[Ch]Cl + oxalic acid	−0.1000	−0.0450
[Ch]Cl + malonic acid	−0.0350	−0.0450
[Ch]Cl + succinic acid	−0.0120	−0.0600
[Ch]Cl + glutaric acid	−0.0175	−0.0200
[Ch]Cl + malic acid	−0.0950	−0.0100
[Ch]Cl + tartaric acid	−0.1270	0.0100
[Ch]Cl + citric acid	−0.0675	

The accuracy of PC-SAFT to describe the SLE data can be evaluated through the deviations between the calculated (T^{calc}) and experimental melting temperatures (T^{exp}). The deviations are reported in terms of average absolute deviation (AAD) given by eq 12, where N is the total number of experimental data points for each system. The AAD was also used as the objective function to be minimized while fitting the binary interaction parameters for each system.

$$\mathrm{AAD(K)} = \frac{1}{N}\sum_{i=1}^{N} |T_i^{calc}(\mathrm{K}) - T_i^{exp}(\mathrm{K})| \quad (12)$$

Figure 4 shows the AAD values obtained between experimental data and ideal-mixture behavior as well as between experimental data and PC-SAFT modeling. As a consequence of the highly nonideal behavior character of the eutectic mixtures studied here, the use of PC-SAFT results in a considerable decrease of the AAD (in a factor of 1.7 up to 6.5) when compared to the ideal solubility curves.

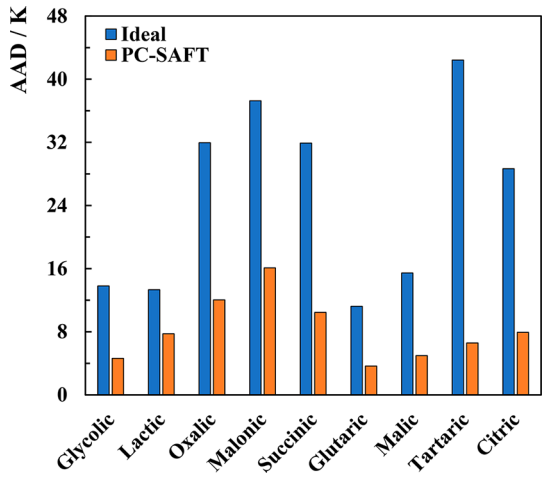

Figure 4. ARD values for melting temperature obtained between experimental data and ideal-mixture behavior as well as between experimental data and PC-SAFT modeling using the parameters in Table 2 and Table 4.

Considering the large temperature intervals involved (more than 300 K), very acceptable deviations of the melting temperatures calculated by PC-SAFT compared to the experimental data (similar to those obtained in our previous works[12,16]) were obtained. The systems presenting higher deviations are those with malonic, oxalic, or succinic acid, which are those presenting melting temperature depressions of higher magnitude and a higher asymmetry; i.e., the salt's solubility curve is fairly ideal while the acid's solubility curve presents significant negative deviations from the ideal behavior (Table S1). In fact, for most systems, PC-SAFT systematically overpredicted the melting temperatures in both solubility curves (and thus the activity coefficients of HBD and HBA). This required the use of negative binary interaction parameters that increase the energy of interaction between the molecules in comparison to the model predictions, which corresponds to a nearly ideal behavior, as depicted in Figure S3. Thus, the obtained values for the fitted binary parameters (Table 4) reinforce the existence of strong interactions between the two components that, ultimately, lead to the formation of a DES. Although both binary interaction parameters can be related to an increase of cross interactions between HBA and HBD, they have a different effect upon the phase behavior of the system. Thus, both the k_{ij}, which increases the cross-dispersive energy, and k_{ij_eps}, increasing the cross-association energies, were required to successfully capture the experimental data. The reason for this was the highly unsymmetrical phase behavior of these systems; i.e., considerably higher deviations from the ideal behavior were observed for the solubility curve of the acid than that of [Ch]Cl.

As it was proven that PC-SAFT provides an accurate description of the experimental phase diagrams over the whole concentration range, it can be further used to assess reliable estimates of the eutectic points. The eutectic point coordinates (x^E_{HBD}, T^E) obtained by PC-SAFT are represented in Figure 5 and reported in Table S3 along with those assuming an ideal behavior. As can be seen in Figure 5A, the eutectic composition of the different DES depends strongly on the kind of carboxylic acid used but, with the exception of the mixture with lactic acid, the eutectic compositions are roughly located in the range from 0.3 to 0.5 of acid mole fractions. A similar trend of the ideal behavior predictions is followed, except for mixtures involving dicarboxylic acids, whose eutectic compositions are considerably higher than those predicted by assuming an ideal behavior. These results show that the eutectic composition on these DESs is mainly controlled by the HBD's chemical structure and rarely corresponds to a fixed HBA/HBD ratio, even for compounds from the same family. This highlights the importance of studying the solid−liquid phase behavior of DESs with special focus on the experimental determination of the whole phase diagram for a correct assessment of the eutectic points, prior to the application of DESs. Moreover, the phase diagrams allow the identification of the compositions that are liquid at operating temperature and thus can be used as solvents.

Similarly, the PC-SAFT estimated eutectic temperatures (Figure 5B) seem to depend on the type of carboxylic acid qualitatively the same as those predicted assuming an ideal liquid phase, although larger discrepancies are observed between PC-SAFT estimated eutectic temperatures, T^E_{EoS}, and those assuming an ideal-mixture behavior, T^E_{ideal}. The

DOI: 10.1021/acs.iecr.8b01249
Ind. Eng. Chem. Res. 2018, 57, 11195−11209

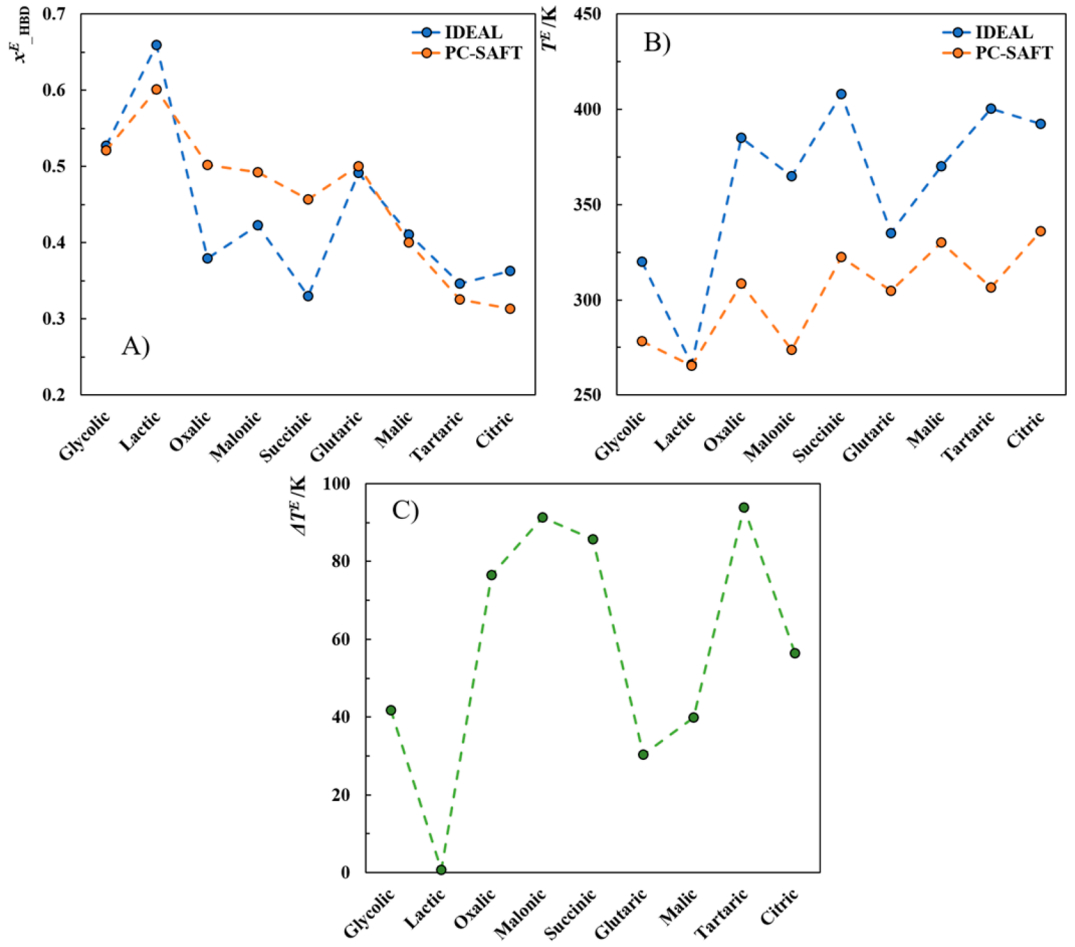

Figure 5. (A) Eutectic compositions (acid mole fraction), (B) eutectic temperatures, (C) melting temperature depressions relatively to the ideal behavior. Blue: eutectic coordinates predicted by the ideal-mixture behavior. Orange: eutectic coordinates estimated with PC-SAFT modeling using the parameters in Table 2 and Table 4.

ideal eutectic temperatures are, as previously shown for eutectic mixtures of [Ch]Cl + fatty acids,[12] mainly determined by the melting temperatures of the pure acids. In contrast, the eutectic temperatures assessed with PC-SAFT suggest that T^E might result from a combined effect of the acid bulk size, the number of functional groups within the HBD, and the molecular interactions between acid molecules. Results clearly show that the eutectic temperatures increase with the HBD's molar volume (e.g., malonic acid < succinic acid < malic acid < citric acid) while they may or may not decrease with the number of functional groups present in the HBD (e.g., tartaric acid < malic acid but succinic acid < malic acid). The effect of the number of functional groups present in the HBD is not straightforward. For instance, the eutectic temperature of the system [Ch]Cl + tartaric acid is lower than that observed for the mixture [Ch]Cl + citric acid, although the melting temperature of pure tartaric acid is 15 K higher than that of citric acid. Both tartaric acid and citric acid contain four functional groups (between hydroxyl and carboxylic groups) able to interact with [Ch]Cl; however, the self-association interactions in the pure acid are much stronger in citric acid than in tartaric acid due to the presence of more COOH−COOH interactions in comparison to the comparatively weaker OH−OH interactions. This is also the reason for the fact that the activity coefficients of tartaric acid (in Figure 3) are lower than those of citric acid, despite that both acids induce similar deviations from ideal behavior on the activity coefficient of [Ch]Cl. These results suggest that although the number of functional groups play a vital role in inducing negative deviations from the ideal behavior in the [Ch]Cl solubility (also highlighted by the nearly ideal behavior of the mixtures with glycolic or lactic acid), both the number and the type of functional groups, and interactions present in the pure HBD, have a strong influence on the solubility of the HBD in the DES and thus on the eutectic temperatures.

The melting temperature depressions ($\Delta T^E = T^E_{ideal} - T^E_{EoS}$) to the ideal behavior predictions are depicted in Figure 5C; values between 0.81 K ([Ch]Cl + lactic acid) and 93.86 K ([Ch]Cl + tartaric acid) can be observed from this figure. The highest melting temperature depressions are observed for the systems with tartaric acid or smaller dicarboxylic acids (oxalic, malonic, or succinic acids). The former benefits from a higher number of functional groups, and from the presence of OH−OH interactions in the pure acid, weaker than those established with [Ch]Cl. However, the smaller dicarboxylic acids benefit from a win−win combination of the different effects: they have a small chain length combined with an optimal number of functional groups, which are just sufficient to prevent positive deviations from ideality in the [Ch]Cl solubility (contrarily to monofunctional HBDs[12]), without considerably increasing the magnitude of self-interactions in the pure HBD as it is the case for citric and malic acids. These

DOI: 10.1021/acs.iecr.8b01249
Ind. Eng. Chem. Res. 2018, 57, 11195−11209

results suggest that the effect of an increasing number of functional groups (which has a positive impact on the [Ch]Cl solubility) is counterbalanced by the stronger interactions established in the pure HBD. Nevertheless, the very large melting temperature depressions observed for most systems allow the formation of stable liquids at low temperatures; the studied mixtures exhibit eutectic temperatures in the range 265.4−336.0 K.

As stated before, the SL phase diagrams of DES are extremely scarce, but extremely important to check the composition range where the binary mixture can be as a stable liquid around room temperature. Regarding the systems investigated here, Abbott et al.[13] presented a few data points of the SLE of mixtures of [Ch]Cl with oxalic, malonic, or succinic acids (Figure 3), and some other (poly)carboxylic acids have been used as HBD to form [Ch]Cl-based DES. Data measured in this work are generally in agreement with the data published by Abbott et al.[13] Both works agree that while [Ch]Cl + malonic acid melts around 274 K at the eutectic composition, [Ch]Cl + succinic or oxalic acids do not form a liquid at room temperature, as it was also stated by Florindo et al.[14] for succinic acid + [Ch]Cl. Conversely, both Florindo et al.[14] and Aroso et al.[69] report the formation of liquids at room temperatures for the DESs [Ch]Cl + citric acid and [Ch]Cl + tartaric acid in different HBD/HBA ratios, while our data indicate a eutectic point around 307 and 336 K for the eutectic mixtures with tartaric and citric acids, respectively. Unfortunately, further discussions on these discrepancies are difficult due to the lack of experimental details, in particular the water content of their mixtures, and the absence of more information on these systems in the open literature.

Densities and viscosities of the eutectic mixtures were determined at atmospheric pressure in the temperature range between 283.15 and 373.15 K and are reported in Figure 6 and Tables S4 and S5 of the Supporting Information, along with the mole fraction of the acids. All mixtures studied are denser than water and both, densities and viscosities decrease with increasing temperature. The mixtures involving lactic and tartaric acids are the less and more dense, respectively. The same is observed for viscosities. In general, the viscosity decreases with the decrease of the number or functional groups: tartaric, citric, and malic acids are more viscous, followed by succinic, glutaric, malonic, and oxalic acids.

The high viscosities of the systems studied are related with the strong hydrogen bonds between the components. Their large size lead to small void volumes and, therefore, lower mobility of the species. As shown before for systems involving sugars,[70] the addition of water to these systems decreases their densities and viscosities due to the formation of a higher number of potential hydrogen bonds between the solutes and water. Thus, this type of system can easily be tuned into systems with enhanced transport properties for industrial applications. However, it should be pointed out that the addition of water strongly influences the phase behavior[71] and thus the phase boundaries should be re-evaluated at the desired water content.

5. CONCLUSIONS

Binary mixtures composed of [Ch]Cl and one of nine (poly)carboxylic acids were prepared and the SL phase diagrams measured using a visual detection technique. Contrarily to the nearly ideal behavior reported for binary mixtures of [Ch]Cl and fatty acids, the systems investigated

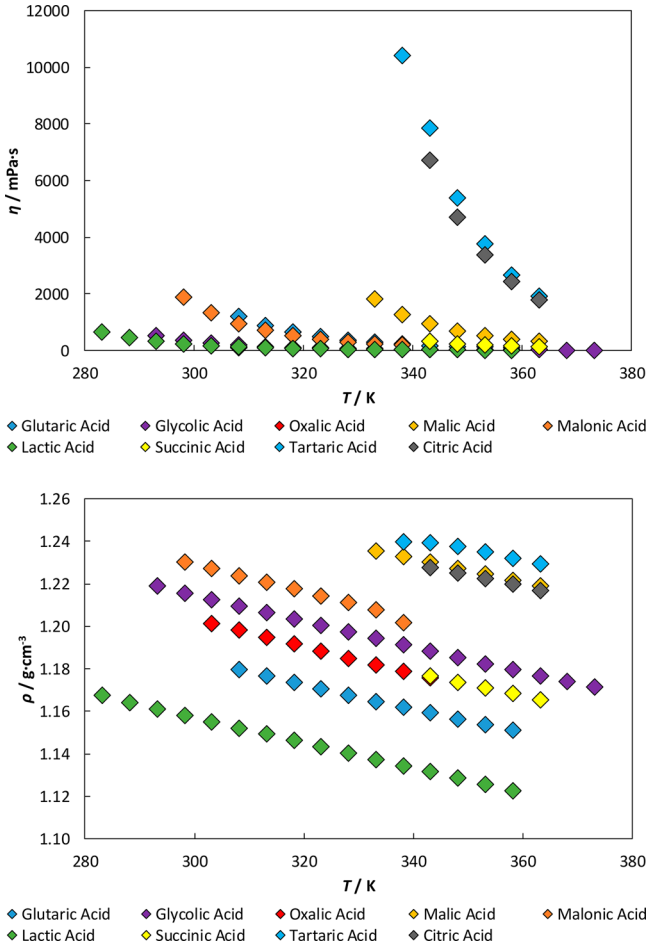

Figure 6. Experimental densities, ρ, and viscosities, η, of the investigated systems (Ch[Cl] + (poly)carboxylic acids) at atmospheric pressure.

here exhibit strong negative deviations from ideality, resulting in considerable melting temperature depressions that may lead to the formation of stable liquids at relatively low temperatures (some even at room temperature). These results highlight the importance of using multifunctional hydrogen bond donors to establish stronger cross-interactions in the mixtures than those observed in the pure compounds.

The experimental phase diagrams were modeled with PC-SAFT, which has been shown to be an accurate tool for the thermodynamic description of the studied DES. The model required a maximum of two temperature-independent binary interaction parameters between HBA and HBD in order to capture the system's physical features. All interaction parameters were found to have negative values highlighting the strong cross-interactions between the DES constituents. An exception was the system with tartaric acid where a positive k_{ij_eps} was required due to the highly negative k_{ij}. Moreover, the model was used to assess the eutectic points coordinates (temperature and composition) that were compared with those expected for an ideal mixture. Similarly to our findings with [Ch]Cl + fatty acids systems, no fixed stoichiometry HBD:HBA was found at the eutectic point. The eutectic temperature depressions were found to result from a combined effect of the bulk size, number and type of functional groups of the HBD. Further systematic studies on the impact of each of

DOI: 10.1021/acs.iecr.8b01249
Ind. Eng. Chem. Res. 2018, 57, 11195−11209

these variables would contribute with fundamental information for an efficient computer-aided design of [Ch]Cl-based DES.

■ ASSOCIATED CONTENT

Supporting Information

The Supporting Information is available free of charge on the ACS Publications website at DOI: 10.1021/acs.iecr.8b01249.

Tables of experimental (x_2, T) and calculated (γ_i) data of the SLE of systems, water content of the eutectic points, eutectic point coordinates, and experimental density and viscosity results; photograph of investigated mixtures at the eutectic composition; ^{1}H NMR spectra; SLE phase diagram (PDF)

■ AUTHOR INFORMATION

Corresponding Author

*J. A. P. Coutinho. E-mail: jcoutinho@ua.pt. Phone: +351 234401507. Fax: +351 234370084.

ORCID

Emanuel A. Crespo: 0000-0003-2137-0564
Mónia A. R. Martins: 0000-0003-0748-1612
Christoph Held: 0000-0003-1074-177X
Simão P. Pinho: 0000-0002-9211-857X
João A. P. Coutinho: 0000-0002-3841-743X

Notes

The authors declare no competing financial interest.

■ ACKNOWLEDGMENTS

This work was developed in the scope of the project CICECO − Aveiro Institute of Materials, POCI-01-0145-FEDER-007679 (ref. FCT UID/CTM/50011/2013) and Associate Laboratory LSRE-LCM, POCI-01-0145-FEDER-006984 (ref. FCT UID/EQU/50020/2013), both financed by national funds through the FCT/MEC and when appropriate cofinanced by FEDER under the PT2020 Partnership Agreement. This work is also a result of project "AlProcMat@N2020 - Advanced Industrial Processes and Materials for a Sustainable Northern Region of Portugal 2020", with the reference NORTE-01-0145-FEDER-000006, supported by Norte Portugal Regional Operational Programme (NORTE 2020), under the Portugal 2020 Partnership Agreement, through the European Regional Development Fund (ERDF). M.A.R.M and E.A.C acknowledge FCT for the Ph.D. grants SFRH/BD/87084/2012 and SFRH/BD/130870/2017, respectively. FCT is also acknowledged for funding the project DeepBiorefinery (PTDC/AGRTEC/1191/2014). C.H. gratefully acknowledges financial support from the Max-Buchner Research Foundation and from German Science Foundation (DFG), grant HE 7165/7-1.

■ REFERENCES

(1) Abbott, A. P.; Capper, G.; Davies, D. L.; Rasheed, R. K.; Tambyrajah, V. Novel Solvent Properties of Choline Chloride/Urea Mixtures. *Chem. Commun.* **2003**, *99* (1), 70−71.

(2) Smith, E. L.; Abbott, A. P.; Ryder, K. S. Deep Eutectic Solvents (DESs) and Their Applications. *Chem. Rev.* **2014**, *114* (21), 11060−11082.

(3) Dai, Y.; van Spronsen, J.; Witkamp, G.-J. J.; Verpoorte, R.; Choi, Y. H. Natural Deep Eutectic Solvents as New Potential Media for Green Technology. *Anal. Chim. Acta* **2013**, *766*, 61−68.

(4) Hayyan, M.; Hashim, M. A.; Hayyan, A.; Al-Saadi, M. A.; AlNashef, I. M.; Mirghani, M. E. S.; Saheed, O. K. Are Deep Eutectic Solvents Benign or Toxic? *Chemosphere* **2013**, *90* (7), 2193−2195.

(5) de Morais, P.; Gonçalves, F.; Coutinho, J. A. P.; Ventura, S. P. M. Ecotoxicity of Cholinium-Based Deep Eutectic Solvents. *ACS Sustainable Chem. Eng.* **2015**, *3* (12), 3398−3404.

(6) Hayyan, M.; Mbous, Y. P.; Looi, C. Y.; Wong, W. F.; Hayyan, A.; Salleh, Z.; Mohd-Ali, O. Natural Deep Eutectic Solvents: Cytotoxic Profile. *Springerplus* **2016**, *5* (1), 913.

(7) Tang, B.; Row, K. H. Recent Developments in Deep Eutectic Solvents in Chemical Sciences. *Monatsh. Chem.* **2013**, *144* (10), 1427−1454.

(8) Morrison, H. G.; Sun, C. C.; Neervannan, S. Characterization of Thermal Behavior of Deep Eutectic Solvents and Their Potential as Drug Solubilization Vehicles. *Int. J. Pharm.* **2009**, *378* (1), 136−139.

(9) Maugeri, Z.; Domínguez de María, P. Novel Choline-Chloride-Based Deep-Eutectic-Solvents with Renewable Hydrogen Bond Donors: Levulinic Acid and Sugar-Based Polyols. *RSC Adv.* **2012**, *2* (2), 421−425.

(10) Shahbaz, K.; Mjalli, F. S.; Hashim, M. A.; Al-Nashef, I. M. Using Deep Eutectic Solvents for the Removal of Glycerol from Palm Oil-Based Biodiesel. *J. Appl. Sci.* **2010**, *10* (24), 3349−3354.

(11) Shahbaz, K.; Mjalli, F. S.; Hashim, Ma.; AlNashef, I. M. Prediction of Deep Eutectic Solvents Densities at Different Temperatures. *Thermochim. Acta* **2011**, *515* (1), 67−72.

(12) Crespo, E. A.; Silva, L. P.; Martins, M. A. R.; Fernandez, L.; Ortega, J.; Ferreira, O.; Sadowski, G.; Held, C.; Pinho, S. P.; Coutinho, J. A. P. Characterization and Modeling of the Liquid Phase of Deep Eutectic Solvents Based on Fatty Acids/Alcohols and Choline Chloride. *Ind. Eng. Chem. Res.* **2017**, *56* (42), 12192−12202.

(13) Abbott, A. P.; Boothby, D.; Capper, G.; Davies, D. L.; Rasheed, R. K. Deep Eutectic Solvents Formed between Choline Chloride and Carboxylic Acids: Versatile Alternatives to Ionic Liquids. *J. Am. Chem. Soc.* **2004**, *126* (29), 9142−9147.

(14) Florindo, C.; Oliveira, F. S.; Rebelo, L. P. N.; Fernandes, A. M.; Marrucho, I. M. Insights into the Synthesis and Properties of Deep Eutectic Solvents Based on Choline Chloride and Carboxylic Acids. *ACS Sustainable Chem. Eng.* **2014**, *2* (10), 2416−2425.

(15) van Osch, D. J. G. P.; Zubeir, L. F.; van den Bruinhorst, A.; Rocha, M. A. A.; Kroon, M. C. Hydrophobic Deep Eutectic Solvents as Water-Immiscible Extractants. *Green Chem.* **2015**, *17* (9), 4518−4521.

(16) Pontes, P. V. A.; Crespo, E. A.; Martins, M. A. R.; Silva, L. P.; Neves, C. M. S. S.; Maximo, G. J.; Hubinger, M. D.; Batista, E. A. C.; Pinho, S. P.; Coutinho, J. A. P.; et al. Measurement and PC-SAFT Modeling of Solid-Liquid Equilibrium of Deep Eutectic Solvents of Quaternary Ammonium Chlorides and Carboxylic Acids. *Fluid Phase Equilib.* **2017**, *448*, 69−80.

(17) Choi, Y. H.; van Spronsen, J.; Dai, Y.; Verberne, M.; Hollmann, F.; Arends, I. W. C. E.; Witkamp, G.-J.; Verpoorte, R. Are Natural Deep Eutectic Solvents the Missing Link in Understanding Cellular Metabolism and Physiology? *Plant Physiol.* **2011**, *156* (4), 1701−1705.

(18) Parnica, J.; Antalik, M. Urea and Guanidine Salts as Novel Components for Deep Eutectic Solvents. *J. Mol. Liq.* **2014**, *197*, 23−26.

(19) Phadtare, S. B.; Shankarling, G. S. Halogenation Reactions in Biodegradable Solvent: Efficient Bromination of Substituted 1-Aminoanthra-9,10-Quinone in Deep Eutectic Solvent (Choline Chloride: Urea). *Green Chem.* **2010**, *12* (3), 458−462.

(20) Pawar, P. M.; Jarag, K. J.; Shankarling, G. S. Environmentally Benign and Energy Efficient Methodology for Condensation: An Interesting Facet to the Classical Perkin Reaction. *Green Chem.* **2011**, *13* (8), 2130−2134.

(21) Azizi, N.; Batebi, E.; Bagherpour, S.; Ghafuri, H. Natural Deep Eutectic Salt Promoted Regioselective Reduction of Epoxides and Carbonyl Compounds. *RSC Adv.* **2012**, *2* (6), 2289−2293.

(22) Abbott, A. P.; Capper, G.; Davies, D. L.; Rasheed, R. K.; Shikotra, P. Selective Extraction of Metals from Mixed Oxide Matrixes

Using Choline-Based Ionic Liquids. *Inorg. Chem.* **2005**, *44* (19), 6497−6499.
(23) Biswas, A.; Shogren, R. L.; Stevenson, D. G.; Willett, J. L.; Bhowmik, P. K. Ionic Liquids as Solvents for Biopolymers: Acylation of Starch and Zein Protein. *Carbohydr. Polym.* **2006**, *66* (4), 546−550.
(24) Abbott, A. P.; Cullis, P. M.; Gibson, M. J.; Harris, R. C.; Raven, E. Extraction of Glycerol from Biodiesel into a Eutectic Based Ionic Liquid. *Green Chem.* **2007**, *9* (8), 868−872.
(25) Zhao, H.; Baker, G. A. Ionic Liquids and Deep Eutectic Solvents for Biodiesel Synthesis: A Review. *J. Chem. Technol. Biotechnol.* **2013**, *88* (1), 3−12.
(26) Garcia, G.; Aparicio, S.; Ullah, R.; Atilhan, M. Deep Eutectic Solvents: Physicochemical Properties and Gas Separation Applications. *Energy Fuels* **2015**, *29*, 2616−2644.
(27) Gross, J.; Sadowski, G. Perturbed-Chain SAFT: An Equation of State Based on a Perturbation Theory for Chain Molecules. *Ind. Eng. Chem. Res.* **2001**, *40* (4), 1244−1260.
(28) Gross, J.; Sadowski, G. Application of the Perturbed-Chain SAFT Equation of State to Associating Systems Application of the Perturbed-Chain SAFT Equation of State To. *Ind. Eng. Chem. Res.* **2002**, *41*, 5510−5515.
(29) Tan, S. P.; Adidharma, H.; Radosz, M. Recent Advances and Applications of Statistical Associating Fluid Theory. *Ind. Eng. Chem. Res.* **2008**, *47* (21), 8063−8082.
(30) Verevkin, S. P.; Sazonova, A. Y.; Frolkova, A. K.; Zaitsau, D. H.; Prikhodko, I. V.; Held, C. Separation Performance of BioRenewable Deep Eutectic Solvents. *Ind. Eng. Chem. Res.* **2015**, *54* (13), 3498−3504.
(31) Zubeir, L. F.; Held, C.; Sadowski, G.; Kroon, M. C. PC-SAFT Modeling of CO2 Solubilities in Deep Eutectic Solvents. *J. Phys. Chem. B* **2016**, *120* (9), 2300−2310.
(32) Lloret, J. O.; Vega, L. F.; Llovell, F. Accurate Description of Thermophysical Properties of Tetraalkylammonium Chloride Deep Eutectic Solvents with the Soft-SAFT Equation of State. *Fluid Phase Equilib.* **2017**, *448*, 81−93.
(33) Fernandez, L.; Silva, L. P.; Martins, M. A. R.; Ferreira, O.; Ortega, J.; Pinho, S. P.; Coutinho, J. A. P. Indirect Assessment of the Fusion Properties of Choline Chloride from Solid-Liquid Equilibria Data. *Fluid Phase Equilib.* **2017**, *448*, 9−14.
(34) Emel'Yanenko, V. N.; Verevkin, S. P.; Stepurko, E. N.; Roganov, G. N.; Georgieva, M. K. Thermodynamic Properties of Glycolic Acid and Glycolide. *Russ. J. Phys. Chem. A* **2010**, *84* (8), 1301−1308.
(35) Domalski, E. S.; Hearing, E. D. Heat Capacities and Entropies of Organic Compounds in the Condensed Phase. Volume III. *J. Phys. Chem. Ref. Data* **1996**, *25* (1), 1−525.
(36) Lange, L.; Schleinitz, M.; Sadowski, G. Predicting the Effect of PH on Stability and Solubility of Polymorphs, Hydrates, and Cocrystals. *Cryst. Growth Des.* **2016**, *16* (7), 4136−4147.
(37) Hansen, A. R.; Beyer, K. D. Experimentally Determined Thermochemical Properties of the Malonic Acid/Water System: Implications for Atmospheric Aerosols. *J. Phys. Chem. A* **2004**, *108* (16), 3457−3466.
(38) Acree, W. E. Thermodynamic Properties of Organic Compounds: Enthalpy of Fusion and Melting Point Temperature Compilation. *Thermochim. Acta* **1991**, *189* (1), 37−56.
(39) Good, D. J.; Rodríguez-Hornedo, N. Solubility Advantage of Pharmaceutical Cocrystals. *Cryst. Growth Des.* **2009**, *9* (5), 2252−2264.
(40) Ceolin, R.; Szwarc, H.; Lepage, F. On the Dimorphism of Dl-Malic Acid. *Thermochim. Acta* **1990**, *158* (2), 347−352.
(41) Meltzer, V.; Pincu, E. Thermodynamic Study of Binary Mixture of Citric Acid and Tartaric Acid. *Open Chem.* **2012**, *10* (5), 1584−1589.
(42) Hendriks, E. M. Applied Thermodynamics in Industry, a Pragmatic Approach. *Fluid Phase Equilib.* **2011**, *311*, 83−92.
(43) Chapman, W. G.; Gubbins, K. E.; Jackson, G.; Radosz, M. New Reference Equation of State for Associating Liquids. *Ind. Eng. Chem. Res.* **1990**, *29* (8), 1709−1721.
(44) Wertheim, M. S. Fluids with Highly Directional Attractive Forces. I. Statistical Thermodynamics. *J. Stat. Phys.* **1984**, *35* (1), 19−34.
(45) Wertheim, M. S. Fluids with Highly Directional Attractive Forces. II. Thermodynamic Perturbation Theory and Integral Equations. *J. Stat. Phys.* **1984**, *35* (1), 35−47.
(46) Wertheim, M. S. Fluids with Highly Directional Attractive Forces. III. Multiple Attraction Sites. *J. Stat. Phys.* **1986**, *42* (3), 459−476.
(47) Wertheim, M. S. Fluids with Highly Directional Attractive Forces. IV. Equilibrium Polymerization. *J. Stat. Phys.* **1986**, *42* (3), 477−492.
(48) Barker, J. A.; Henderson, D. Perturbation Theory and Equation of State for Fluids: The Square-Well Potential. *J. Chem. Phys.* **1967**, *47* (8), 2856−2861.
(49) Barker, J. A.; Henderson, D. Perturbation Theory and Equation of State for Fluids. II. A Successful Theory of Liquids. *J. Chem. Phys.* **1967**, *47* (11), 4714−4721.
(50) Wolbach, J. P.; Sandler, S. I. Using Molecular Orbital Calculations To Describe the Phase Behavior of Cross-Associating Mixtures. *Ind. Eng. Chem. Res.* **1998**, *37* (8), 2917−2928.
(51) Gross, J.; Sadowski, G. Application of the Perturbed-Chain SAFT Equation of State to Associating Systems. *Ind. Eng. Chem. Res.* **2002**, *41*, 5510−5515.
(52) Ji, X.; Held, C.; Sadowski, G. Modeling Imidazolium-Based Ionic Liquids with EPC-SAFT. *Fluid Phase Equilib.* **2012**, *335*, 64−73.
(53) Nann, A.; Mündges, J.; Held, C.; Verevkin, S. P.; Sadowski, G. Molecular Interactions in 1-Butanol + IL Solutions by Measuring and Modeling Activity Coefficients. *J. Phys. Chem. B* **2013**, *117* (11), 3173−3185.
(54) Passos, H.; Khan, I.; Mutelet, F.; Oliveira, M. B.; Carvalho, P. J.; Santos, L. M. N. B. F.; Held, C.; Sadowski, G.; Freire, M. G.; Coutinho, J. A. P. Vapor-Liquid Equilibria of Water plus Alkylimidazolium-Based Ionic Liquids: Measurements and Perturbed-Chain Statistical Associating Fluid Theory Modeling. *Ind. Eng. Chem. Res.* **2014**, *53* (9), 3737−3748.
(55) Huang, S. H.; Radosz, M. Equation of State for Small, Large, Polydisperse and Associating Molecules. *Ind. Eng. Chem. Res.* **1990**, *29*, 2284−2294.
(56) Albers, K.; Heilig, M.; Sadowski, G. Reducing the Amount of PCP−SAFT Fitting Parameters. 2. Associating Components. *Fluid Phase Equilib.* **2012**, *326*, 31−44.
(57) Kleiner, M.; Tumakaka, F.; Sadowski, G. Thermodynamic Modeling of Complex Systems. In *Molecular Thermodynamics of Complex Systems*; Lu, X., Hu, Y., Eds.; Springer: Berlin, Heidelberg, 2009; pp 75−108.
(58) Riedel, L. Eine Neue Universelle Dampfdruckformel Untersuchungen Über Eine Erweiterung Des Theorems Der Übereinstimmenden Zustände. Teil I. *Chem. Ing. Tech.* **1954**, *26* (2), 83−89.
(59) Lange, L.; Sadowski, G. Thermodynamic Modeling for Efficient Cocrystal Formation. *Cryst. Growth Des.* **2015**, *15* (9), 4406−4416.
(60) Lange, L.; Lehmkemper, K.; Sadowski, G. Predicting the Aqueous Solubility of Pharmaceutical Cocrystals As a Function of PH and Temperature. *Cryst. Growth Des.* **2016**, *16* (5), 2726−2740.
(61) Daubert, T. E.; Sibul, H. M.; Stebbins, C. C.; Danner, R. P.; Rowley, R. L.; Adams, M. E.; Wilding, W. V; Marshall, T. L. *Physical and Thermodynamic Properties of Pure Chemicals: DIPPR: Data Compilation: Core + Supplements 1−10*; Taylor & Francis, 2000.
(62) Abbott, M. M.; Smith, J. M.; Van Ness, H. C. *Introduction to Chemical Engineering Thermodynamics*; McGraw-Hill, 2001.
(63) Martins, M. A. R.; Pinho, S. P.; Coutinho, J. A. P. Insights into the Nature of Eutectic and Deep Eutectic Mixtures. *J. Solution Chem.* **2018**, in press.
(64) Collin, R. L. POLYMORPHISM AND RADIATION DECOMPOSITION OF CHOLINE CHLORIDE1. *J. Am. Chem. Soc.* **1957**, *79* (22), 6086.
(65) Shanley, P.; Collin, R. L. The Crystal Structure of the High Temperature Form of Choline Chloride. *Acta Crystallogr.* **1961**, *14* (1), 79−80.

DOI: 10.1021/acs.iecr.8b01249
Ind. Eng. Chem. Res. 2018, 57, 11195−11209

(66) Petropavlov, N. N.; Tsygankova, I. G.; Teslenko, L. A. Microcalorimetric Investigation of Polymorphic Transitions in Organic Crystals. *Sov. Phys. Crystallogr.* **1988**, *33* (6), 853−855.
(67) Fukai, M.; Matsuo, T.; Suga, H. Thermodynamic Properties of Phase Transitions in Malonic Acid and Its Deuterated Analogue. *Thermochim. Acta* **1991**, *183*, 215−243.
(68) Cingolani, A.; Berchiesi, G. Thermodynamic Properties of Organic Compounds. *J. Therm. Anal.* **1974**, *6* (1), 87−90.
(69) Aroso, I. M.; Paiva, A.; Reis, R. L.; Duarte, A. R. C. Natural Deep Eutectic Solvents from Choline Chloride and Betaine − Physicochemical Properties. *J. Mol. Liq.* **2017**, *241*, 654−661.
(70) Silva, L. P.; Fernández, L.; Conceição, J. H. F.; Martins, M. A. R.; Sosa, A.; Ortega, J.; Pinho, S. P.; Coutinho, J. A. P. Design and Characterization of Sugar-Based Deep Eutectic Solvents Using COSMO-RS. *ACS Sustainable. Chem. Eng.* **2018**, DOI: 10.1021/acssuschemeng.8b02042.
(71) Meng, X.; Ballerat-Busserolles, K.; Husson, P.; Andanson, J.-M. Impact of Water on the Melting Temperature of Urea + Choline Chloride Deep Eutectic Solvent. *New J. Chem.* **2016**, *40* (5), 4492−4499.

DOI: 10.1021/acs.iecr.8b01249
Ind. Eng. Chem. Res. 2018, 57, 11195−11209